Biochemistry and Chemical Biology
Cell Biology

A tool to pulse-label yeast Nuclear Pore Complexes in imaging and biochemical experiments

Reviewed Preprint
v1 • September 9, 2025
Not revised

Annemiek C Veldsink, Jonas S Fischer, Sophie Hell, Karsten Weis, Liesbeth M Veenhoff

European Research Institute for the Biology of Ageing, University of Groningen, University Medical Center Groningen, Groningen, Netherlands • Institute of Biochemistry, Department of Biology, ETH Zurich, Zurich, Switzerland

eLife Assessment

This **valuable** study introduces a non-perturbative pulse-labeling strategy for yeast nuclear pore complexes (NPCs), employing a nanobody-based approach in order to selectively capture Nup84-containing complexes for imaging and biochemical analysis. The data **convincingly** demonstrate that a short induction period (20 minutes to 1 hour) yields a strong and sustained signal, enabling affinity purification that faithfully recapitulates the endogenous Nup84 interactome. This tool offers a powerful framework for investigating NPC dynamics and associated interactomes through both imaging and biochemical assays.

https://doi.org/10.7554/eLife.108399.1.sa3

Abstract

Summary

Nuclear Pore Complexes (NPCs) are key gateways to the nucleus and major organizers of genome architecture. Despite their importance, it is still not fully understood how NPCs are formed and degraded. Tools to track specific NPCs over time or under stress could unlock critical insights into these questions. Here, we demonstrate that a brief pulse of expression of a previously developed nanobody against baker's yeast nucleoporin Nup84 (Nordeen et al. 2020) enables a robust, rapid, and straightforward method for pulse-labeling NPCs in both imaging and affinity purification experiments. This approach offers an alternative to permanent yet less rapid genetic fluorophore- or tag-switching techniques and provides a powerful tool for studying NPC inheritance and turnover through both microscopy and biochemical methods.

Rapid labeling of NPCs using a nanobody against Nup84

Single domain antibodies, nanobodies, have been developed for structural biology (Nordeen et al. 2020), for protein purifications (Stankunas and Köhler 2024) and for probing *in vivo* protein assemblies (Solà Colom et al. 2024). A previously developed nanobody (VHH) against the yeast nucleoporin (Nup) Nup84 (Nordeen et al. 2020), a conserved member of the outer ring structures of NPCs, binds Nup84 with nanomolar affinity (VHH-SAN8, from here on VHH[Nup84]) (Nordeen et al. 2020). To examine the use of VHH[Nup84] as a tool to fluorescently pulse-label NPCs, we fused it to mNeongreen (mNG), a bright fluorophore with short maturation times in yeast (Guerra et al. 2022). We placed the construct under an inducible galactose promotor, allowing for time-controlled expression bursts (**Fig. 1A**), albeit with some cell-to cell and experimental variability in the expression levels. Expression of VHH[Nup84]-mNG did not affect cell viability or growth rates, as also previously shown (Nordeen et al. 2020). We observed colocalization of VHH[Nup84]-mNG with NPCs marked by the endogenously tagged NPC component Pom34-mCh (**Fig. 1B**) and no detectable NE signal was observed in Nup84Δ cells (**Fig. 1C**), confirming previous structural studies showing that VHH[Nup84] specifically binds Nup84 (Nordeen et al. 2020). Noteworthy, a short, 20-minute expression burst was enough to give a detectable NE signal till at least two hours after the initial induction (**Fig. 1B,D**). Quantifying the signal, we measure that in the first two hours after a 20-minute expression pulse, the mean intensity of VHH[Nup84] reached approximately 46% +/-27% of the intensity of endogenously tagged Nup84 (**Fig. 1E**). A longer induction pulse of 1hr further increased the labeling of NPCs compared to a 20-minute expression pulse and the fluorescence levels become indistinguishable (108% +/-33%) from those obtained with endogenously tagged Nup84 (**Fig. 1D,E**). Given that the NE labeling intensities are ultimately determined by both incorporation of new VHH[Nup84]-mNG into NPCs as well as the dilution of labeled NPCs to daughter cells, it makes sense that the maximal labeling intensities measured follow the division times in minimal medium (+/-2hrs) (**Fig. 1E**). Collectively, these findings show that pulse-labeling Nup84 in NPCs is quick and tunable, providing an alternative to endogenous tagging of NPC subunits.

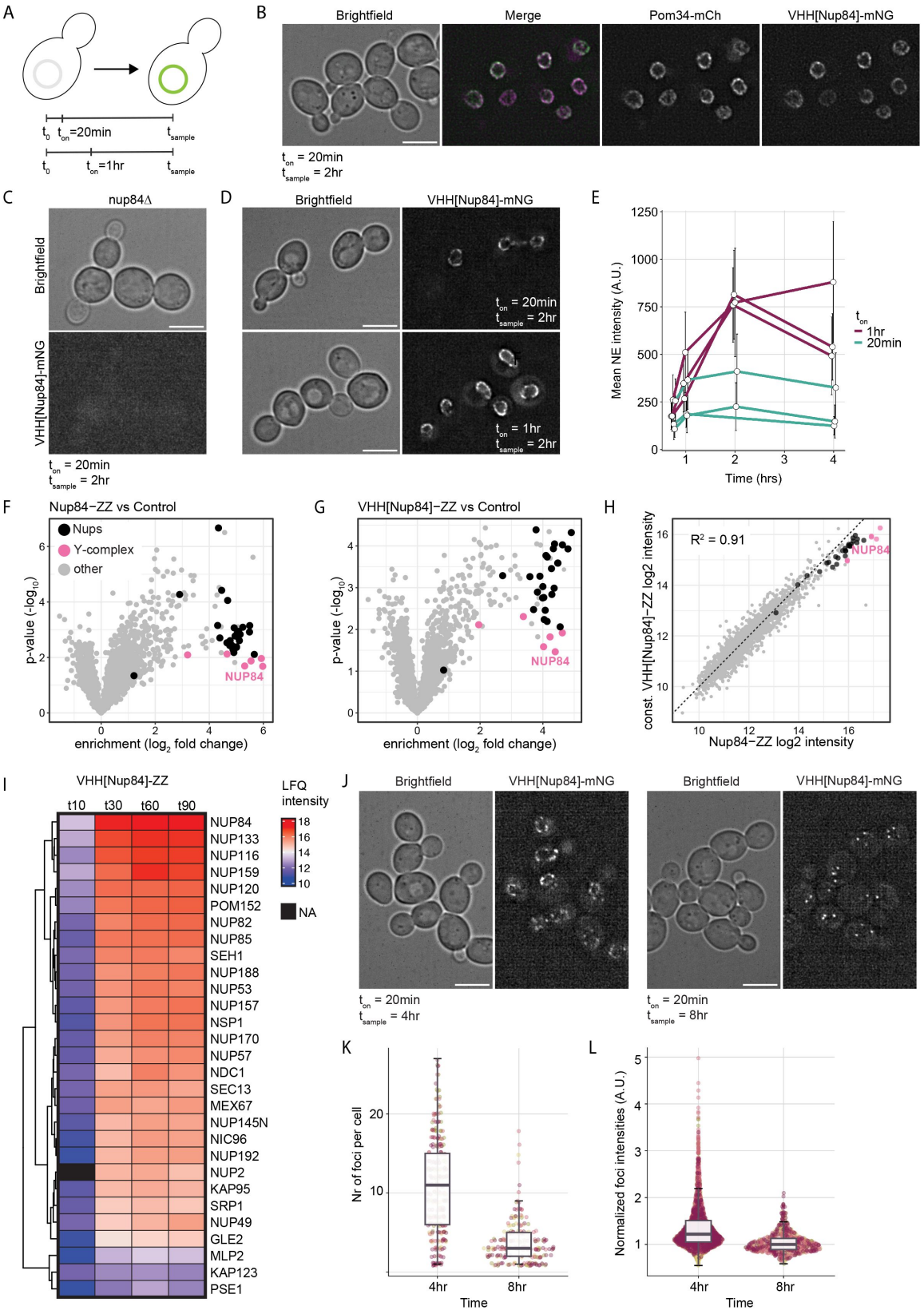
A
B
Brightfield
Merge
Pom34-mCh
VHH[Nup84]-mNG
C
nup84Δ
Brightfield
VHH[Nup84]-mNG
D
E
Mean NE intensity (A.U.)
Time (hrs)
F
Nup84−ZZ vs Control
Nups
Y-complex
other
p-value (-log10)
enrichment (log2 fold change)
G
VHH[Nup84]−ZZ vs Control
H
R2 = 0.91
const. VHH[Nup84]−ZZ log2 intensity
Nup84−ZZ log2 intensity
I
VHH[Nup84]-ZZ
t10
t30
t60
t90
LFQ intensity
NA
NUP84
NUP133
NUP116
NUP159
NUP120
POM152
NUP82
NUP85
SEH1
NUP188
NUP53
NUP157
NSP1
NUP170
NUP57
NDC1
SEC13
MEX67
NUP145N
NIC96
NUP192
NUP2
KAP95
SRP1
NUP49
GLE2
MLP2
KAP123
PSE1
J
K
Nr of foci per cell
4hr
8hr
Time
L
Normalized foci intensities (A.U.)

Fig. 1.

Nanobody against Nup84 is a tool to pulse-label yeast NPCs in imaging and biochemical experiments

A) Schematic of the experimental set-up. At t_0, VHH[Nup84]-mNG is expressed for the specified amount of time (t_{on}) by addition of 0.5% galactose to the medium. Expression is subsequently shut off by addition of 1% glucose and images are taken at time (t_{sample}) to determine NPC labeling.

B) Colocalization of VHH[Nup84]-mNG with Pom34-mCh at t=2hr following a 20min induction pulse. Images represent summed projections of 3 z-slices (midplane +/- 0.5 µm). Scale bar = 5 µm.

C) Typical image of VHH[Nup84]-mNG in nup84Δ cells at t=2hr following a 20min induction pulse. Images represent a single z-slice. Scale bar = 5 µm

D) Typical images of VHH[Nup84]-mNG at t=2hr following either a 20min or 1hr induction pulse. Images represent sum projections of 3 z-slices (midplane +/- 0.1 µm). Scale bar = 5 µm.

E) Quantification of NE intensities in the midplane of cells at various timepoints following a 20min (cyan) or 1hr (purple) induction pulse. Data represents mean NE intensity +/- standard deviation of three biological replicas. Numbers of cells analyzed (t_{on} - t_{sample}): 102 (20min-45min), 139 (20min-1hr), 82 (20min-2hr, *N=2*), 92 (20min-4hr), 111 (1hr-45min), 186 (1hr-1hr), 153 (1hr-2hr), 193 (1hr-4hr). Mean NE intensity +/- standard deviation of endogenously tagged Nup84-mNG is 726 +/-148 (224 cells).

F) Volcano plot showing the log2 fold enrichment of proteins in affinity purifications using endogenously expressed Nup84-ZZ as a bait compared to mock-ZZ. Nups are colored in black, the Nup84 subcomplex is colored in magenta.

G) Volcano plot showing the log2 fold enrichment of proteins in affinity purifications using VHH[Nup84]- ZZ constitutively expressed from the Nup120 promotor as a bait compared to mock-ZZ. Nups are colored in black, the Nup84 subcomplex is colored in magenta.

H) Correlation between protein intensities in the affinity purifications with VHH[Nup84] from **F** and **G**.

I) Heat map showing log2 intensities of Nups and NTRs in VHH[Nup84]-ZZ affinity purifications at the various sampling timepoints following a 20 min VHH[Nup84] induction pulse. LFQ = label free quantitation.

J) Typical image of the localization of VHH[Nup84]-mNG at t=4hr and t=8hr following a 20-minute induction pulse. Each panel represents a sum projection of 5 consecutive z-slices (0.1 µm). Scale bar = 5 µm.

K) Quantification of the number of VHH[Nup84]-mNG foci per cell at t=4hr and t=8hr following a 20- minute induction pulse. Each dot represents a cell, each color reflects a biological replica. Boxplots represent median and first and third quartiles, whiskers extend to 1.5x IQR. Nr of cells analyzed (t_{on} - t_{sam}ple): 289 (20min-4hr), 215 (20min-8hr) from four biological replicas.

L) Intensities of detected VHH[Nup84]-mNG foci at t=4hr and t=8hr following a 20-minute induction pulse. Intensities are normalized to median foci intensity at t=8hr of the corresponding replica. Each dot represents a single focus, each color reflects a biological replica. Boxplots represent median and first and third quartiles, whiskers extend to 1.5x IQR. Nr of cells analyzed (t_{on} - t_{sample}): 289 (20 min-4 hr), 215 (20min-8hr) from four biological replicas.

VHH[Nup84]-ZZ is a suitable bait for NPC affinity purifications

In addition to the use of VHH[Nup84]-mNG as a pulse-labeling tool in imaging experiments, we characterized the value of ZZ-tagged VHH[Nup84] as a bait in affinity purifications (APs) of NPCs using IgG-coated beads. We constitutively expressed VHH[Nup84] from the Nup120 promotor and found that all Nups significantly coenriched with VHH[Nup84]-ZZ as compared to control APs in cells expressing a free ZZ-tag (**Fig. 1G**). Importantly, the level to which Nups are enriched is comparable to APs with endogenously tagged Nup84-ZZ (**Fig. 1F**) and overall, there is a strong correlation between APs using the VHH[Nup84]-ZZ and the Nup84-ZZ baits (R2 = 0.91) (**Fig. 1H**). This demonstrates that VHH[Nup84] can be used as an affinity bait to purify NPCs, on par with endogenously tagged Nup84-ZZ.

Next, we set out to investigate the affinity purification efficiency of VHH[Nup84]-ZZ when used to pulse-label NPCs. We used a short, 20-minute induction burst to express the VHH[Nup84]-ZZ bait and subsequently determined its interactome at various timepoints (**Fig. 1I**). This short expression pulse was enough to specifically purify NPCs 1.5 hours after the induction (**Fig. 1I**) and we could already confidently identify most Nups 10 minutes after the start of bait expression. Their intensity increased at the 30 min timepoint and did not drastically change 1.5 hours after labeling start (**Fig. 1I**). This indicates that pulse-labeling is very fast and that VHH[Nup84]-ZZ stays stably bound to the NPC over longer times. Hence, VHH[Nup84]-ZZ can be a powerful tool to pulse-label NPCs to assess the interactome of NPCs at specific points in time.

VHH[Nup84] can be used to trace labeled NPCs in time

Considering that exchange of individual Nups, including Nup84, is generally slow with half times in the order of hours (Hakhverdyan et al. 2021; Rabut, Doye, and Ellenberg 2004), we wondered whether we could use VHH[Nup84] pulse-labeling to follow labeled NPCs over longer time periods. Using the same experimental set-up described in **Fig. 1A,we** imaged cells 4hrs and 8hrs after the short 20 min induction pulse. At 8hrs, the signal was diluted from NE rings (**Fig. 1B,D**) to individual foci (**Fig. 1J**), indeed indicating the inheritance of labeled NPCs to daughter cells in mitosis. To quantify the number of foci per cell, we employed the PunctaFinder plugin that can detect foci in 3D (Terpstra et al. 2024). Between 4 and 8hrs, the median number of foci per cell decreased from 11 to 3 (**Fig. 1K**), which is consistent with cell cycle kinetics and a previous reports showing that approximately 40% of the existing NPCs are transmitted to the daughter cell in each division (Zsok et al. 2024; Khmelinskii et al. 2010). The spread in foci intensities decreased in time (**Fig. 1L**), which is likely related to the high density of >10 NPC/µm2 NE (Winey et al. 1997) that compromises the detection of individual pores when they are all labeled. The median intensity reduced by approximately 20% between 4 and 8hrs (**Fig. 1L**), consistent with the stable association of VHH[Nup84] with NPCs. Considering that the rapid labeling of NPCs leads to a quick depletion of unbound VHH[Nup84]-mNG from the cytosol, these foci very likely reflect NPCs that were labeled in the early time stages. Thus, VHH[Nup84]-mNG allows the visualization and tracking of individual NPC over time.

Altogether, we show that VHH[Nup84] is a tool for pulse-labeling of NPCs in live yeast cells in imaging and biochemical experiments. The pulse-labeling of Nup84 in NPCs with VHH[Nic96]-mNG is quick and tunable, providing an alternative to endogenous tagging of NPC subunits. Amongst others this is useful in conditions where direct tagging of Nup84 interferes with its

function, while sub stoichiometric nanobody binding does not. The binding of VHH[Nic96]-mNG with NPCs is quick and stable and hence allows the imaging of individual NPCs in time over multiple divisions. Pulsed expression of VHH[Nic96] thus provides an alternative to the recombination-induced tag exchange (RITE) cassette or optically switchable fluorophores (Verzijlbergen et al. 2010; Zsok et al. 2024; Onischenko et al. 2020; Toyama et al. 2019; Colombi et al. 2013; Zhou and Lin 2013). Lasty, ZZ-tagged VHH[Nup84] can be used as an affinity bait to purify NPCs, on par with endogenously tagged Nup84-ZZ, and, when expressed shortly it can be used to assess the interactome of NPCs at specific points in time or under specific conditions.

As NPCs are long-lived structures, VHH[Nup84] may specifically allow for NPC inheritance studies or the characterization of aged NPCs that were labeled early on during the experiment. Along the same line, we envision that applying genetic perturbations or environmental stresses such as oxidizing conditions, heat stress or osmotic shock at the time of VHH[Nup84] pulse-labeling, provides a means to study the long-term fate of these NPCs. For example, this could resolve the question whether these NPCs are specifically degraded. Similarly, we envision that VHH[Nup84] pulse-labeling strategies can also be used to inducible bring specific proteins in proximity of NPC, e.g. for determining the local and time resolved interactome of NPCs using proximity labeling strategies (Filali-Mouncef et al. 2024). These and other future studies tracking NPC inheritance and studying NPC turnover mechanisms might uncover how the quality of NPCs in maintained and how this fails in ageing and disease.

Methods

Yeast strains and growth

All strains used in this study are listed in **Table 1**. Strains were generated using standard microbiology techniques and validated by microscopy and/or PCR. For all pulse-labeling experiments, strains were inoculated 2 days prior to the experiment and grown in synthetic minimal medium supplemented with 2% D-glucose (30°C, 200rpm). On day -1, cells were diluted in minimal medium supplemented with 2% D-raffinose and grown to exponential phase, maintaining them in mid-exponential phase from this point onwards. At the start of the experiment, VHH[Nup84] expression was induced by addition of 0.5% galactose to the medium (2% in the affinity purification experiment; panel I), followed by addition of 1% glucose (2% in the affinity purification experiment; panel I) after 20 minutes or 1hr as described in the figure.

Fluorescence microscopy

Images were acquired using a Deltavision Elite (Applied Precision) microscope, using an Olympus UPlanSApo 100x (NA 1.4) oil immersion objective and equipped with an EDGE sCMOS5.5 camera for detection. Images were acquired in 30 Z-slices of 0.1 µm, except for panel B (3 z-slices of 0.5 µm). SoftWoRx software (GE Healthcare) was used for image deconvolution and images were processed using Fiji software (ImageJ 2.14.0) (Schindelin et al. 2012). NE intensities were measured in Fiji by drawing lines cans over the NE in the midplane and correcting for background intensity. Dumbbell shaped NEs or cells without visible NE staining were excluded from analysis, as were cells in which lines cans could not be confidently drawn.

Affinity purifications and proteomic data acquisition and analysis

Proteomic experiments and data analysis were essentially performed as described in (Kralt et al 2022). To induce expression of VHH bait, cells were grown to mid-log phase as described above and then transferred from medium containing 2% raffinose to medium containing 2% galactose.

Yeast strains		
Name	***Genotype***	***Description / source***
W303	MATa leu2-3,112 trp1-1 can1-100 ura3-1 ade2-1 his3-11,15	Open Biosystems
yAV108	W303; Leu2::pGal1-VHH[Nup84]-mNeongreen	VHH[Nup84]-mNG under galactose promotor integrated in the Leu2 locus using pAV49
yAV115	yAV108; Pom34-mCherry::URA3	C-terminal tagging of Pom34-mCherry using pPP014 (Popken et al. 2015)
yAV178	yAV108; Nup84Δ::Hyg	Deletion of Nup84 using pFA6-HphNT1
yAV213	yAV108; Lys2Δ::KanMX, Leu2::pGal1-VHH[Nup84]-S-TEV-ZZ::HIS3	VHH[Nup84]-S-TEV-ZZ under galactose promotor integrated in the Leu2 locus with HIS3 selection marker, using pKW803 to replace mNG with S-TEV-ZZ. Lys2 deletion by PCR amplification of lys2 deletion cassette from YKO collection
KWY12171	Lys2Δ::KanMX His3::pNup120-VHH[Nup84]-S-TEV-ZZ	Constitutively expressed pNup120-VHH[Nup84]-S-TEV-ZZ in the His3 locus
KWY12149	Lys2Δ::KanMX Nup84-S-TEV-ZZ::His3	(Onischenko et al. 2017)

Plasmids		
Name	***Description***	***Source***
pRS305	Integrative vector with LEU2 marker	Addgene (Markus, Punch, and Lee 2009)
pPP014	PCR template for C-terminal mCherry tagging; URA3 selection	(Rempel et al. 2019)
pFA6-HphNT1	Gene deletion cassette; hygromycin resistance	(Janke et al. 2004)
pKW803	pFA6-S-TEV-ZZ; HIS3 selection	(Onischenko et al. 2017)
pAV49	pGal1-VHH[Nup84]-mNeongreen-Cyc in pRS305 backbone	This study

Table 1.

Strains and plasmids

After 20 minutes of induction, bait expression was halted by directly adding 2% glucose (v/v). At the specified timepoints, samples equivalent to 250 mL of culture of OD600 of 1 were harvested by filtration and snap-frozen in liquid nitrogen.

All steps of the affinity purification protocol were performed on ice, minimizing delays to maintain protein complex integrity. Frozen yeast pellets were resuspended in lysis buffer (20 mM HEPES pH 7.5, 50 mM KOAc, 20 mM NaCl, 2 mM MgCl2, 1 mM DTT, 10% v/v glycerol) and transferred to 2 mL screwcap microtubes (Sarstedt Inc.) pre-filled with ~1 mL of 0.5 mm glass beads (BioSpec Products). The tubes were topped up with additional lysis buffer, and cells were lysed mechanically using a Mini BeadBeater-24 (BioSpec Products) in four 1-minute cycles at 3500 oscillations per minute, with 1-minute cooling intervals in ice water between cycles. Cell debris and unlysed cells were pelleted at 850 x g for 30 s at 4°C and 1 mL of the resulting supernatant was supplemented with 110 µL 10× detergent mix (protease inhibitor cocktail [Sigma-Aldrich], 5% v/v Triton x-100, 1% v/v Tween-20 in lysis buffer). This mixture was transferred to a fresh tube with 1 mg IgG-coated pre-equilibrated magnetic beads (Invitrogen Dynabeads M-270 Epoxy #14301; Sigma rabbit IgG serum #I5006). Samples were incubated at 4°C for 30 minutes with continuous mixing. Beads were then washed four times with 1 mL of wash buffer (0.1% v/v Tween-20 in lysis buffer) and bound proteins were eluted in 40 µL of 1× Laemmli sample buffer for 2 minutes at 50°C. Eluates were then denatured at 95°C for 5 minutes.

Proteins were concentrated by SDS-PAGE using a 4% acrylamide stacking gel, then incubated in distilled water for 12 hours to remove residual detergents. Protein bands were excised and processed using a standard in-gel digestion protocol. In brief, disulfide bonds were reduced with dithiothreitol (6.5 mM DTT in 100 mM ammonium bicarbonate) for 1 hour at 60°C, followed by alkylation with iodoacetamide (54 mM in 100 mM ammonium bicarbonate) for 30 minutes at 30°C in the dark. Proteins were then digested with 1.25 µg trypsin (Promega) in 100 mM ammonium bicarbonate for 16 h at 37°C. Peptides were desalted using C18 BioPureSPN mini columns (The Nest Group, Inc), washed with Buffer A (0.1% v/v formic acid), eluted with Buffer B (0.1% v/v formic acid, 80% v/v acetonitrile), and ultimately recovered in 12.5 µL Buffer A supplemented with iRT peptides (1:50 v/v, Biognosys).

LC-MS/MS analysis was performed on an Orbitrap Exploris 480 mass spectrometer (Thermo Scientific) coupled to a Vanquish Neo UHPLC system (Thermo Scientific). Peptide separation was achieved on a C18 reversed-phase column (75 µm x 400 mm (New Objective), packed in-house with ReproSil Gold 120 C18, 1.9 µm (Dr. Maisch GmbH)). For the time course samples with the inducible VHH[Nup84] construct, peptides were eluted using a 120-minute linear gradient from 7% to 35% buffer B (0.1% [v/v] formic acid, 80% [v/v] acetonitrile) at a flow rate of 300 nl/min. The mass spectrometer was operated in data-independent acquisition (DIA) mode using one MS1 scan (350-1150 m/z, 120000 resolution, 250% normalized AGC target, 264 ms maximum injection time), followed by 41 variable MS2 windows from 350-1150 m/z with 1 m/z overlap (30000 resolution, 250% normalized AGC target, 64 ms maximum injection time). Fragmentation was carried out by HCD at normalized collision energy (NCD) 28%. For constitutively expressed VHH[Nup84] samples, a 60-minute non-linear gradient from 1% to 43.7% buffer B at a flow rate of 300 nl/min was used. DIA was performed with one MS1 scan (330-1650 m/z, 120000 resolution, 300% normalized AGC target, 20 ms maximum injection time), followed by 30 variable MS2 windows from 330 to 1650 m/z with 1 m/z overlap (30000 resolution, 2000% normalized AGC target, 64 ms maximum injection time). Fragmentation was also performed using HCD, with NCE set to 27%.

The data from the time course samples were extracted with Spectronaut v18.2 (Biognosys) using a spectral library previously generated from 60 APs with 11 Nup baits (Kralt et al. 2022). Data from constitutively expressed VHH[Nup84] were extracted with Spectronaut v19.1 using the directDIA workflow. Carbamidomethylation was used as fixed modification and methionine oxidation, and N-terminal acetylation were set as variable modifications. Tryptic peptides with less than two missed cleavages were considered, and spectra were searched against the

Saccharomyces cerevisiae protein database (downloaded from SGD on 13/10/2015, 6713 entries). For DIA data analysis in Spectronaut, all default settings were kept except that "cross-run normalization" was turned off. The ion intensities at the fragment level were exported and analysed in R as follows: First, low-quality precursors were excluded based on Spectronaut's "F. ExcludedFromQuantification" flag. All remaining fragment ions with an intensity > 4 were were summed. Only prototypic precursors were retained and precursor intensities were summarized into protein intensities using the MaxLFQ method (Cox et al. 2014). Proteins with less than three identified precursor ions in all three replicates were filtered out. Protein intensities were median normalized per sample, and the mean of three biological replicates was used as the final protein intensity. Statistical significance was assessed using a two-tailed Student's t-test. The samples with inducible VHH[Nup84] were originally acquired using SILAC with isotopically labelled lysine. However, for our analysis, we relied on label-free quantification by summing the ion intensities of heavy and light y-type fragment ions from precursors containing a single lysine.

PunctaFinder analysis

PunctaFinder analysis(Terpstra et al. 2024) (panels K, L) was essentially performed as described in Veldsink et al. 2025, using the same threshold settings (T_{local} = 1.47 (ratio punctum/surroundings) and T_{global} = 1.83 (ratio punctum/cell)). Subsequent filtering steps were omitted as the absence of cytosolic VHH[Nup84]-mNG pools did not require additional filtering of detected puncta. Output was analyzed using R software version 4.1.0 (RCoreTeam; 2024). For median normalization of foci intensities (panel L), intensities of all foci at t=4hrs and t=8hrs were divided by the median foci intensity at t=8hr of the same replica.

Graphs and statistics

Graphs and statistical analysis were performed using R software version 4.1.0 (RCoreTeam; 2024).

Acknowledgements

We kindly thank Prof. Dr. Thomas Schwartz (MIT) for sharing the Nup84 nanobody. We thank Federico Uliana and Ino D Karemaker from the IBC MS facility. We thank Michael Chang all members of the Chang and Veenhoff labs for valuable input. Annemiek Veldsink was supported by a PhD-fellowships from the Graduate School of Medical Sciences of the University of Groningen. This work was supported by a Vici grant (VI.C.192.031) to LMV from the Netherlands Organisation for Scientific Research and funding to KW from the Swiss National Science Foundation (TMAG-3_209354 CRSII5_193740).

Additional information

Author contribution

Conception and design: ACV, JSF, KW, LMV; Acquisition of data: ACV, JSF SH; Analysis and interpretation of data: ACV, JSF; Drafting and revising the article: ACV, JSF, KW, LMV

Materials and Correspondence

Materials and correspondence may be addressed to Liesbeth Veenhoff

Note

This reviewed preprint has been updated to correct level headings.

References

Colombi Paolo, Webster Brant M., Fröhlich Florian, Lusk C. Patrick (2013) **The transmission of nuclear pore complexes to daughter cells requires a cytoplasmic pool of Nsp1** *Journal of Cell Biology* **203**:215–32 Google Scholar

Cox J., Hein M. Y., Luber C. A., Paron I., Nagaraj N., Mann M. (2014) **Accurate proteome-wide label-free quantification by delayed normalization and maximal peptide ratio extraction, termed MaxLFQ** *Mol Cell Proteomics* **13**:2513–26 Google Scholar

Filali-Mouncef Y., Leytens A., Duarte P. Vargas, Zampieri M., Dengjel J., Reggiori F. (2024) **An APEX2-based proximity-dependent biotinylation assay with temporal specificity to study protein interactions during autophagy in the yeast Saccharomyces cerevisiae** *Autophagy* **20**:2323–37 Google Scholar

Guerra Paolo, Vuillemenot Luc-Alban, Rae Brady, Ladyhina Valeriia, Milias-Argeitis Andreas (2022) **Systematic In Vivo Characterization of Fluorescent Protein Maturation in Budding Yeast** *ACS Synthetic Biology* **11**:1129–41 Google Scholar

Hakhverdyan Z., Molloy K. R., Keegan S., Herricks T., Lepore D. M., Munson M., Subbotin R. I., Fenyo D., Aitchison J. D., Fernandez-Martinez J., Chait B. T., Rout M. P. (2021) **Dissecting the Structural Dynamics of the Nuclear Pore Complex** *Mol Cell* **81**:153–65 Google Scholar

Janke C., Magiera M. M., Rathfelder N., Taxis C., Reber S., Maekawa H., Moreno-Borchart A., Doenges G., Schwob E., Schiebel E., Knop M. (2004) **A versatile toolbox for PCR-based tagging of yeast genes: new fluorescent proteins, more markers and promoter substitution cassettes** *Yeast* **21**:947–62 Google Scholar

Khmelinskii Anton, Keller Philipp J., Lorenz Holger, Schiebel Elmar, Knop Michael (2010) **Segregation of yeast nuclear pores** *Nature* **466**:E1–E1 Google Scholar

Kralt A., Wojtynek M., Fischer J. S., Agote-Aran A., Mancini R., Dultz E., Noor E., Uliana F., Tatarek-Nossol M., Antonin W., Onischenko E., Medalia O., Weis K. (2022) **An amphipathic helix in Brl1 is required for nuclear pore complex biogenesis in S. cerevisiae** *eLife* **11** Google Scholar

Markus S. M., Punch J. J., Lee W. L. (2009) **Motor- and tail-dependent targeting of dynein to microtubule plus ends and the cell cortex** *Curr Biol* **19**:196–205 Google Scholar

Nordeen S. A., Andersen K. R., Knockenhauer K. E., Ingram J. R., Ploegh H. L., Schwartz T. U. (2020) **A nanobody suite for yeast scaffold nucleoporins provides details of the nuclear pore complex structure** *Nat Commun* **11**:6179 Google Scholar

Onischenko E., Noor E., Fischer J. S., Gillet L., Wojtynek M., Vallotton P., Weis K. (2020) **Maturation Kinetics of a Multiprotein Complex Revealed by Metabolic Labeling** *Cell* **183**:1785–800 Google Scholar

Onischenko E., Tang J. H., Andersen K. R., Knockenhauer K. E., Vallotton P., Derrer C. P., Kralt A., Mugler C. F., Chan L. Y., Schwartz T. U., Weis K. (2017) **Natively Unfolded FG Repeats Stabilize the Structure of the Nuclear Pore Complex** *Cell* **171**:904–17 Google Scholar

Popken Petra, Ghavami Ali, Onck Patrick R., Poolman Bert, Veenhoff Liesbeth M. (2015) **Size-dependent leak of soluble and membrane proteins through the yeast nuclear pore complex** *Molecular Biology of the Cell* **26**:1386–94 Google Scholar

Rabut Gwénaël, Doye Valérie, Ellenberg Jan (2004) **Mapping the dynamic organization of the nuclear pore complex inside single living cells** *Nature Cell Biology* **6**:1114–21 Google Scholar

RCoreTeam (2024) **R: A Language and Environment for Statistical Computing** Vienna, Austria: R Foundation for Statistical Computing

Rempel Irina L., Crane Matthew M., Thaller David J., Mishra Ankur, Jansen Daniel P. M., Janssens Georges, Popken Petra, Aksit Arman, Kaeberlein Matt, van der Giessen Erik, Steen Anton, Onck Patrick R., Lusk C. Patrick, Veenhoff Liesbeth M. (2019) **Age-dependent deterioration of nuclear pore assembly in mitotic cells decreases transport dynamics** *eLife* **8**:1–26 Google Scholar

Schindelin Johannes, Arganda-Carreras Ignacio, Frise Erwin, Kaynig Verena, Longair Mark, Pietzsch Tobias, Preibisch Stephan, Rueden Curtis, Saalfeld Stephan, Schmid Benjamin, Tinevez Jean-Yves, White Daniel James, Hartenstein Volker, Eliceiri Kevin, Tomancak Pavel, Cardona Albert (2012) **Fiji: an open-source platform for biological-image analysis** *Nature Methods* **9**:676–82 Google Scholar

Solà Colom M., Fu Z., Gunkel P., Güttler T., Trakhanov S., Srinivasan V., Gregor K., Pleiner T., Görlich D. (2024) **A checkpoint function for Nup98 in nuclear pore formation suggested by novel inhibitory nanobodies** *EMBO J* **43**:2198–232 Google Scholar

Stankunas E., Köhler A. (2024) **Docking a flexible basket onto the core of the nuclear pore complex** *Nat Cell Biol* **26**:1504–19 Google Scholar

Terpstra H. M., Gómez-Sánchez R., Veldsink A. C., Otto T. A., Veenhoff L. M., Heinemann M. (2024) **PunctaFinder: An algorithm for automated spot detection in fluorescence microscopy images** *Mol Biol Cell* **35**:mr9 Google Scholar

Toyama Brandon H., Drigo Rafael Arrojoe, Lev-Ram Varda, Ramachandra Ranjan, Deerinck Tomas J., Lechene Claude, Ellisman Mark H., Hetzer Martin W. (2019) **Visualization of long-lived proteins reveals age mosaicism within nuclei of postmitotic cells** *Journal of Cell Biology* **218**:433–44 Google Scholar

Verzijlbergen K. F., Menendez-Benito V., van Welsem T., van Deventer S. J., Lindstrom D. L., Ovaa H., Neefjes J., Gottschling D. E., van Leeuwen F. (2010) **Recombination-induced tag exchange to track old and new proteins** *Proc Natl Acad Sci U S A* **107**:64–8 Google Scholar

Winey M., Yarar D., Giddings T. H., Mastronarde D. N. (1997) **Nuclear pore complex number and distribution throughout the Saccharomyces cerevisiae cell cycle by three-dimensional reconstruction from electron micrographs of nuclear envelopes** *Mol Biol Cell* **8**:2119–32 Google Scholar

Zhou X. X., Lin M. Z. (2013) **Photoswitchable fluorescent proteins: ten years of colorful chemistry and exciting applications** *Curr Opin Chem Biol* **17**:682–90 Google Scholar

Zsok J., Simon F., Bayrak G., Isaki L., Kerff N., Kicheva Y., Wolstenholme A., Weiss L. E., Dultz E. (2024) **Nuclear basket proteins regulate the distribution and mobility of nuclear pore complexes in budding yeast** *Mol Biol Cell* **35**:ar143 Google Scholar

Author information

Annemiek C Veldsink
European Research Institute for the Biology of Ageing, University of Groningen, University Medical Center Groningen, Groningen, Netherlands

Jonas S Fischer
Institute of Biochemistry, Department of Biology, ETH Zurich, Zurich, Switzerland

Sophie Hell
Institute of Biochemistry, Department of Biology, ETH Zurich, Zurich, Switzerland

Karsten Weis
Institute of Biochemistry, Department of Biology, ETH Zurich, Zurich, Switzerland
ORCID iD: 0000-0001-7224-925X

Liesbeth M Veenhoff
European Research Institute for the Biology of Ageing, University of Groningen, University Medical Center Groningen, Groningen, Netherlands
ORCID iD: 0000-0002-0158-4728

For correspondence: l.m.veenhoff@rug.nl

Editors

Reviewing Editor
Elçin Ünal
University of California, Berkeley, Berkeley, United States of America

Senior Editor
Adèle Marston
University of Edinburgh, Edinburgh, United Kingdom

Reviewer #1 (Public review):

Summary:

The authors present a nanobody-based pulse-labeling system to track yeast NPCs. Transient expression of a nanobody targeting Nup84 (fused to NeonGreen or an affinity tag) permits selective visualization and biochemical capture of NPCs. Short induction effectively labels NPCs, and the resulting purifications match those from conventional Nup84 tagging. Crucially, when induction is repressed, dilution of the labeled pool through successive cell cycles allows the visualization of "old" NPCs (and potentially individual NPCs), providing a powerful view of NPC lifespan and turnover without permanently modifying a core scaffold protein.

Strengths:

(1) A brief expression pulse labels NPCs, and subsequent repression allows dilution-based tracking of older (and possibly single) NPCs over multiple cell cycles.

(2) The affinity-purified complexes closely match known Nup84-associated proteins, indicating specificity and supporting utility for proteomics.

Weaknesses:

(1) Reliance on GAL induction introduces metabolic shifts (raffinose → galactose → glucose) that could subtly alter cell physiology or the kinetics of NPC assembly. Alternative induction systems (e.g., β-estradiol-responsive GAL4-ER-VP16) could be discussed as a way to avoid carbon-source changes.

(2) While proteomics is solid, a comprehensive supplementary table listing all identified proteins (with enrichment and statistics) would enhance transparency.

(3) Importantly, the authors note that the method is particularly useful "in conditions where direct tagging of Nup84 interferes with its function, while sub-stoichiometric nanobody binding does not." After this sentence, it would be valuable to add concrete examples, such as experiments examining NPC integrity in aging or stress conditions where epitope tags can exacerbate phenotypes. These examples will help readers identify situations in which this approach offers clear advantages.

https://doi.org/10.7554/eLife.108399.1.sa2

Reviewer #2 (Public review):

Summary:

This preprint describes a practical and useful approach for labeling and tracking NPCs in situ. While useful applications including timelapse imaging, affinity purification, or proximity labeling are envisioned, addressing some outstanding technical questions would give a clearer picture of the sensitivity and temporal resolution of this approach.

Strengths:

Clever use of a fluorescently conjugated nanobody that binds directly to the core scaffold nucleoporin Nup84 with nanomolar affinity.

Weaknesses:

The decrease in nanobody labeling over 8 hours of chase period is interpreted to indicate that NPCs turn over during this time. However, it is also possible that the nanobody:Nup84 association is disrupted during mitosis by phosphorylation, other PTMs, or structural remodeling.

https://doi.org/10.7554/eLife.108399.1.sa1

Reviewer #3 (Public review):

Summary:

Submitted to the Tools and Resources series, this study reports on the use of a single-domain antibody targeting the nucleoporin Nup84 to probe and track NPCs in budding yeast. The

authors demonstrate their ability to rapidly label or pull down NPCs by inducing the expression of a tagged version of the nanobody (Figure 1).

Strengths:

This tool's main strength is its versatility as an inexpensive, easy-to-set-up alternative to metabolic labelling or optical switching. This same rationale could, in principle, be applied to the study of other multiprotein complexes using similar strategies, provided that single-chain antibodies are available.

Weaknesses:

This approach has no inherent weaknesses, but it would be useful for the authors to verify that their pulse labelling strategy can also be used to detect assembly intermediates, structural variants, or damaged NPCs.

Overall, the data clearly show that Nup84 nanobodies are a valuable tool for imaging NPC dynamics and investigating their interactomes through affinity purification.

https://doi.org/10.7554/eLife.108399.1.sa0